Calibration and correction of LBA/TRMM Abracos pasture site merged dataset

Alan K. Betts
and
John H. Ball
Atmospheric Research
Pittsford, VT 05763

Jose D. Fuentes
Dept. of Environmental Sciences,
Univ. of Virginia
Charlottesville, VA 22903

Version Date 6/13/2002

1. Introduction

This document summarizes the meteorological and gas analyzer data collected by the surface site, and the tethered balloon at the Abracos pasture site during the LBA/TRMM/WETAMC campaign, January-February, 1999. The intercomparison and correction of the data is then discussed. Merged datasets for the surface micromet and gas analyzer, and for the surface micromet and tethered balloon have been produced. Several papers have used these data in preliminary form (Betts et al., 2002a,b; Betts and Jakob, 2002; Silva Dias et al., 2002; Williams et al., 2002).

The main accomplishment is to reduce the relative mean biases between different humidity measurements [Microclimate, gas analyzer and dew point hygrometer, abbreviated MC, GA and DPH] to about ± 1%. There remain some uncertainties in the absolute calibration of both GA and DPH instruments against a dew point generator reference standard. Consequently, we believe that the absolute calibration accuracy of the humidity data may only be ±1-2% in RH. This is however far superior to the accuracy of conventional RH sensors. An error of ± 1% in RH near noon, corresponds to ±3 hPa in cloud-base, and to slightly less than ±1K in θ_E. This is sufficient to give a corrected dataset, that is extremely valuable for the study of boundary layer and convective processes over Rondônia in the rainy season.

Instrument acronyms:
MC: Microclimate station
GA: Gas analyzer
DPH: Dew point hygrometer
TB: tethered balloon with instrument packages: SOND#1, SOND#2, SOND#3
DOY: UTC Time as a decimal fraction of [UTC] Day-of-year, used to identify data ranges/instrument changes. Example: 24.75 is 1800UTC on Jan 24, 1999.
LT: Local time =UTC-4h. Original data had LT timestamp; corrected date has both, and we shall use UTC in this document.

Site Location: Ouro Preto d'Oeste, Rondônia, Brazil; 10^o 45' S, 62^o 22'W, elevation 293m.

2. Measurements

2.1 Micromet tower [TRMM]

Original Timebase: Local Time, LT=UTC-4h
Sampling time for pressure, temperature, humidity, wind and radiation was 2sec.
Averaging interval : 1-min, time-stamp at end of averaging interval.

Table 1. Micrometeorological measurements made at the pasture site.

Measurement	Level	Instrument
T_{soil}	1, 5, 20, 50 cm depth	Thermocouple
Atmospheric pressure	2 m	Pressure transducer
T_{air}	0.5, 1.5, 3, 6, 9.5 m	Ventilated thermistor
T_{air}, RH	1, 6 m	Ventilated thermistor/hygristor
Vapor pressure, CO_2	0.5, 1.5, 4 and 9.5 m	Gas analyzer (model LI-6262, LiCor)
Dew point	6 m	Chilled mirror hygrometer (General Eastern)
Wind speed, direction	10 m	Propeller anemometer (RM Young 05305)
Wind speed (u, v, w)	6 m	3-D Sonic anemometer (model K12, Gill)
Incoming solar radiation Reflected solar radiation	1.5 m 1.5 m	Pyranometer (model PSP, Eppley), 2 instruments Pyranometer (model CM3, Kipp and Zonen)
Incoming longwave radiation Outgoing longwave radiation	1.5 m 1.5 m	Pyrgeometer (model CG3, Kipp and Zonen) Pyrgeometer (model CG3, Kipp and Zonen)
Incoming PAR Outgoing PAR	1.5 m 1.5 m	Quantum sensor (model LI-190SA, LiCor) Quantum sensor (model LI-190SA, LiCor)
Soil Heat flux	5 cm depth	Plates (model 2QS, REBS)
Rainfall amount and intensity	Ground level	Tipping bucket (model TB4, Campbell Scientific)

Known problems [and their solution]
MC wind direction was averaged from 2sec samples up to 1-min, giving erroneous values when wind swings through north. [Solution: Large standard deviation of 1-min mean can be used to identify erroneous values and recompute corrected wind estimate]
Ventilated thermistor/hygristor at 6m appears to have ventilation problems. [This appears to affect mixing ratio only just after sunrise and after rain]
Ventilated thermistor/hygristor at 1m: hygristor appears to have a dry RH bias. [This is correctable]
Gas analyzer lines had condensation at night until DOY = 46.19 when they were heated. Heating reduced on 52.44. [Daytime data mostly reliable]
Dew point hygrometer had line leak till DOY= 36. [Good data after this date, but upward drift of instrument near end of experiment]

2.2 Tethersonde [TRMM]

Timebase: Local Time LT=UTC-4h
Sampling interval : 2-sec

Table 2. Tethersonde measurements made at the pasture site.

Measurement	Level	Instrument
Atmospheric pressure	10 m, ascent, descent	Pressure transducer
T_{air}, RH	10 m, ascent, descent	thermistor/hygristor [Ventilated by wind]
Wind speed, magnetic direction	10 m, ascent, descent	Cup anemometer; geopotentiometer

Operation.
The sonde was tethered at 10m, the height of the top of the tower, for 10mins before and after each ascent/descent profile for cross-calibration against the micromet tower. For the last period with SOND#3, the tether height for these calibration runs was reduced to 6m.

Ascent/descent profiles were made every 3h to coincide with each rawinsonde launch, usually starting 30min before the nominal launch times of 00, 03, 06, 09, 12, 15, 18, and 21 UTC.

Three tethersondes were used
SOND#1 from DOY 21 to 24.75
SOND#2 for 24.75 to 55.56
SOND#3 after DOY= 55.56

Known problems [and their solution].

TB has high T_{air} bias at low wind-speeds (<1.5m s^{-1}) in sunlight due to poor ventilation. [Partial solution: 2 sec winds filtered to remove low wind-speeds in daytime]
TB has residual warm bias in daytime for wind-speeds <4 ms^{-1}, relative to the 9.5m T_{air}. [A correction was applied.]
The three sondes have different bias corrections in pressure, temperature , humidity and wind direction relative to the micromet tower [bias corrections determined and applied]

2.3 Rawinsonde [RA at Abracos site]

Measured T_{air}, RH every 2s on ascent.
GPS measured position, and from this wind was computed every 50sec..
Some sondes measured pressure; some retrieved it from GPS height z and the hydrostatic equation.

Known problems
Surface data in field at Abracos pasture site had surface wind-speed high by factor of 2.
VIZ software interpolated wind-speed, from position values every 50 sec, so intermediate winds are in error, especially when wind swings through north. [Solution: winds were recalculated by interpolation

correct u,v values every 50 secs]
Satellite ephemeris information was incorrect, so GPS had lock-in difficulties and on many occasions sondes were left on ground for GPS lock. Afternoon [1800UTC; 1400LT] sondes often show dry near-surface bias, with mixing ratio increasing in first 100hPa, suggesting a sonde heating problem before launch. [No solution: generally tethersonde data better in BL during daytime]
VIZ humidity known to be wetter than the Vaisala humidity [at LBA sites, RM and RJ]
*These data are not at present included with this dataset***.**

3. Correction of Micromet data

3.1 Micromet wind

3.1.1 Wind speed

The wind speed values in the original archive were high by a factor of 2. These high values also went into the RA sonde data in the field [see corrected sonde data]

3.1.2 Correction of the 1-min wind direction

The issue

The data logger averaged thirty 2-sec values of magnetic wind direction (WD) to give a 1-min mean. This introduces spurious mean values, whenever the wind fluctuates around North, which is more than 10% of the time. Fortunately this also gives a large standard deviation (SdWD), so the bad WD averages can be identified and to first order corrected.

Table 1 shows the frequency distribution in bins of 20 deg of SdWD (columns) and WD (rows), showing the clear separation of the erroneous means from "good" data. Most 1-min averages have a SdWD<20, almost all have <40 deg. There is an arc with large values of SdWD, corresponding to the averaging across north, and very little data has an SD in between. For example, 1-min mean WD in the range 140-220 degrees with 160<SdWD<180 clearly result from averaging roughly equal numbers of WD values with WD slightly west and east of north.

Table 1. Statistics of SdWD in 20 deg bins of WD and SdWD for Jan, 1999.

Summary: @COUNT Field: SdWD
Rows: WD Columns: SdWD*

	0 TO 20	20 T	40 T	60 T	80 T	100	120	140	160	ALL
0 TO 20	4908	3	0	1	0	0	0	0	0	4912
20 TO 40	2543	24	6	55	318	3	0	0	0	2949
40 TO 60	1499	35	1	18	114	251	5	0	0	1923
60 TO 80	1006	41	8	18	10	83	170	21	0	1357
80 TO 100	935	41	11	7	5	11	109	117	0	1236
100 TO 120	1143	50	4	2	5	5	9	175	32	1425
120 TO 140	1336	59	7	4	2	5	9	74	118	1614
140 TO 160	999	59	6	7	1	11	9	26	206	1324
160 TO 180	901	56	10	9	2	3	3	18	224	1226
180 TO 200	1107	48	7	2	7	3	4	21	204	1403
200 TO 220	1382	57	5	6	3	4	4	36	201	1698
220 TO 240	1688	54	8	2	2	7	7	106	106	1980
240 TO 260	1705	54	3	5	7	8	20	212	1	2015
260 TO 280	1614	56	5	6	3	12	180	48	0	1924

280 TO 300	2026	47	4	16	11	202	100	9	0	2415
300 TO 320	2475	44	3	40	264	190	2	0	0	3018
320 TO 340	3226	9	3	97	228	0	0	0	0	3563
340 -- 360	1138	1	0	0	0	0	0	0	0	1139
ALL	33177	738	91	295	982	798	631	863	1092	38667
FILTERED	0	0	0	256	964	777	626	861	1092	4576

Filter for Bad Averages.

The arc of bad data were identified by defining as erroneous all 1-min data that had [SdWD >60 AND SdWD >WD-30] OR [SdWD >60 AND SdWD >360-WD-30]

The bottom line in Table 1 shows the number of data points picked up by this filter.

Estimate of Corrected Wind Direction

The location of a mean along the arc of bad data in Table 1 is determined by the number of 2-sec samples on each side of north. So we then calculated from the erroneous WD mean, a non-integer estimate of the number NN of values to the west of north as

NN= 30*WD/360

Then we made a simple linear estimate of the true mean wind direction, either side of north, based on NN, by roughly fitting a line to the slope of the cumulative distribution with a SD =10 deg [characteristic of the larger dataset].

NN<15, WDcorr = (15-NN)*10/15
NN>15, WDcorr = 360- (NN-15)*10/15)

The logic here is that if NN=15, half the 2-sec values are to the east and half to the west of north, and so north is the best estimate of the wind direction. This probably gives slightly too tight a distribution (spanning less than 350 to 10 degrees, but having used the high SdWD to identify bad data, we have no good estimates of true SdWD. Needless to say, this estimate of WDcorr is far superior to the original mean of the 2-sec values, which scatter over the entire 360^{o} range [see figure xx later].

Table 2 shows a sample of the corrected data. The data with non-zero values of NN [which have the large SdWD values] have been corrected. The last 2 columns show the corrected V component and that calculated from the erroneous WD. The spurious southerly [and easterly] winds have disappeared (shown in red).

Table 2 Example of corrected WD.

MC-DOY,	MC-UTC,	WV ,	WD,	SdWD,	NN,	WDcorr,	Ucorr,	Vcorr,	Verror
25,	1700,	1.5,	152.0,	160.8,	12.7,	1.6,	-0.0,	-1.5,	1.3
25,	1701,	2.0,	168.0,	167.7,	14.0,	0.7,	-0.0,	-2.0,	2.0
25,	1702,	2.6,	147.8,	165.7,	12.3,	1.8,	-0.1,	-2.6,	2.2
25,	1703,	3.3,	22.5,	12.7,	,	22.5,	-1.3,	-3.0,	-3.0
25,	1704,	4.1,	37.5,	11.0,	,	37.5,	-2.5,	-3.2,	-3.2
25,	1705,	3.5,	38.6,	5.2,	,	38.6,	-2.2,	-2.8,	-2.8
25,	1706,	2.4,	41.7,	9.5,	,	41.7,	-1.6,	-1.8,	-1.8

```
25,   1707,    2.4,   41.0,   85.4,    3.4,    7.7,   -0.3,   -2.3,   -1.8
25,   1708,    2.3,  202.0,  153.2,   16.8,  358.8,    0.0,   -2.3,    2.2
25,   1709,    1.8,   25.3,   15.1,       ,   25.3,   -0.8,   -1.7,   -1.7
25,   1710,    2.8,   26.2,   11.4,       ,   26.2,   -1.3,   -2.5,   -2.5
25,   1711,    3.3,   18.5,    7.0,       ,   18.5,   -1.0,   -3.1,   -3.1
25,   1712,    2.1,  208.4,  162.6,   17.4,  358.4,    0.1,   -2.1,    1.8
25,   1713,    1.8,  314.2,   79.3,   26.2,  352.5,    0.2,   -1.8,   -1.2
25,   1714,    2.2,   58.8,   80.3,    4.9,    6.7,   -0.3,   -2.2,   -1.1
25,   1715,    2.7,   55.6,   80.4,    4.6,    6.9,   -0.3,   -2.7,   -1.5
25,   1716,    3.7,   25.3,    9.8,       ,   25.3,   -1.6,   -3.3,   -3.3
25,   1717,    3.3,   18.6,    7.6,       ,   18.6,   -1.0,   -3.1,   -3.1
```

Figure 1 shows the V-component of the wind before and after correction compared to the corresponding 1-min mean wind component from the tethersonde (when tethered by the tower). The correction removes essentially all the spurious southerly wind component values, shown in red.

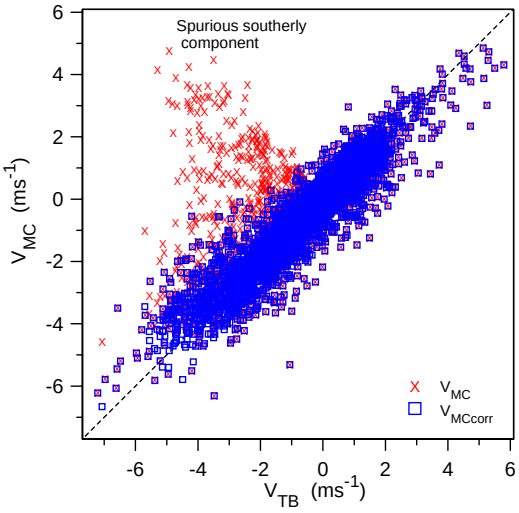

Figure 1. Comparison of v-component of wind from TB and MC, before and after correcting MC wind direction errors.

4. Micromet and gas analyzer comparison.

4.1 Comparison of temperature, mixing ratio and LCL height

We intercompare four sets of instruments
a) a profile of thermisters at 0.5, 1.5, 3, 6 and 9.5m
b) the two probes measuring T and RH at 1 and 6m
c) the gas analyzer [GA] profile of mixing ratio Q at 0.5, 1.5, 4 and 9.5m
d) the dew point hygrometer [DPH] at 6m, measuring dewpoint and therefore vapor pressure and mixing ratio.

In every 10-min interval, the gas analyzer takes a 2-min sample at each of the four levels, with 30-sec between each sample to flush the tubes. We assigned the mid-time of the 10-min time block to all four samples and compared with a 10-min mean of the micromet data for the same 10-min time block. This gave six comparison values per hour with nominal centered times of 5, 15, 25, 35, 45,and 55 mins past the hour. The DPH data, sampled at 1-min, was also averaged to 10-min means to simplify comparison. Because the GA samples are all at different times within the 10-min

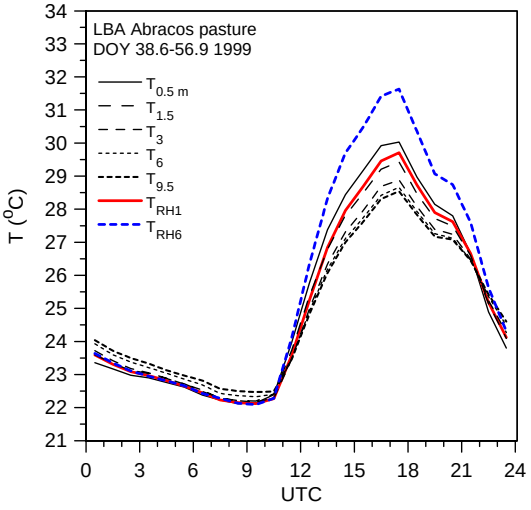

Figure 2. Mean diurnal cycle of temperature from the thermister profile.

time interval, some of the variance in the differences from the MC and DPH data comes from this inhomogeneous sampling. However, when data is averaged up to the hourly timescale, this gives a reasonable estimate of the mean gradients within the surface layer, as well as the mean biases.

In the next few figures, the data has been binned into hourly averages, excluding all data for any 10-min time period where any is missing. Figure 2 shows the mean diurnal cycle of temperature. The five black curves are the profile (a), and they form a smooth progression showing a superadiabatic layer in the daytime (morning though the temperature maximum) and a stable near-surface layer at night. Laboratory intercomparison of these sensors showed they agreed to ± 0.1K, and these mean diurnal profiles are consistent with these sensors having little relative bias. We shall use them as our reference set without correction. The red curve is for the temperature on the 1m (T, RH) probe and in the daytime, it lies between the curves corresponding to 0.5 and 1.5m, suggesting it too has little bias. However the blue dotted curve for the 6m (T, RH) probe is much warmer in the daytime: the sensor had an intermittent ventilation fan which led to a solar heating problem. This is shown clearly in Figure 3, which shows the mean difference in temperature between the thermister in the humidity probes and the corresponding profile thermister: binned in 1ms^{-1} wind speed intervals and for three ranges of incoming solar radiation: <10, 10-500 and >500 W m^{-2}. (We logarithmically averaged the temperatures at 0.5 and 1.5m to give a representative temperature at 1m from the thermister profile.) For the humidity probe at 6m the positive bias reaches 4K at low wind speeds and high incident solar radiation, while the humidity probe at 1-m has little bias at all radiation levels. We believe this was due to a defective fan, giving poor ventilation of the 6-m humidity probe. However, despite the large temperature bias, we shall find the 6-m probe gives a value of mixing ratio, with a correctable bias, except when the sensor is wet, which is primarily just after sunrise.

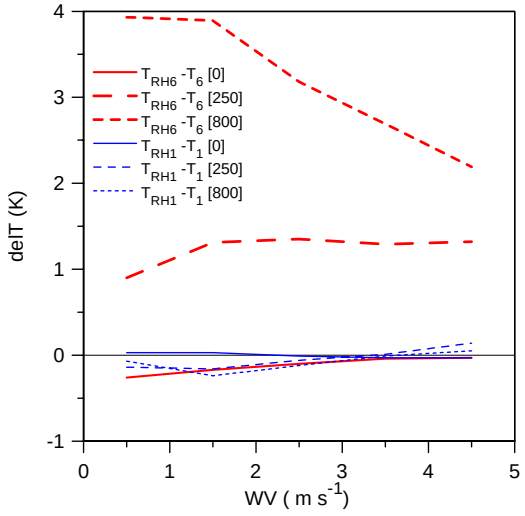

Figure 3. Difference in temperature between RH-probe temperatures and corresponding thermister temperatures, binned by wind speed and incoming solar radiation.

Figure 4 shows in black the mixing ratio, Q, at four levels from the gas analyzer profile. They are measured by cycling air through tubes from different levels though the same instrument during each 10-min interval. They form a regular progression consistent with a superadiabatic layer in the daytime, shown in Figure 2. The red curve is derived from the 1-m (T, RH) probe without any correction. The 1-m probe is about 1.0 to 1.8 g kg^{-1} drier than the GA at a similar level in the daytime. It was clear this RH instrument had a low calibration bias, as it did not saturate at night. The blue dotted curve is Q derived from the 6-m (T, RH) probe: it is about 0.5-1 g kg^{-1} wetter in the daytime than the GA at a similar

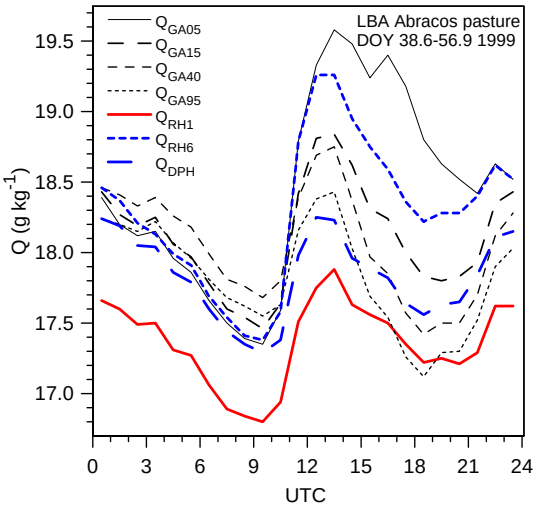

Figure 4. Diurnal cycle of mixing ratio from 4 GA levels, 2 RH-probes and DPH.

level, and rises more sharply after sunrise. The final heavy dashed blue curve is from the DPH: it lies closer to the GA (for the 4-m and 9.5-m levels) than the MC 6-m RH sensor, but has a different diurnal signature. There is thus a range of uncertainty in the uncorrected Q measurements of at least ± 1 g kg^{-1} in the daytime, corresponding to at least ±3% in RH.

4.2 Strategy for correcting the humidity data.

The MC RH-probes give continuous 1-min data for the whole experiment, but clearly have significant biases with respect to the GA data. We need to correct the RH-probe data to give a basis for calibration for the TB-sonde data (there are three different sondes). The GA data enables us to intercompare the 1-m and 6-m RH-probe data, as the same instrument sequentially samples air from both levels. The GA and DPH are both calibrated against a dew-point generator, but the absolute accuracy of this calibration is not well known. The GA calibration is stable, provided temperature and pressure, which determine density, are controlled. We have no control over the surface pressure [the semi-diurnal pressure wave has an amplitude of ±2hPa at this latitude], but this is only a small correction to density. However, because of power problems, the temperature of the LiCor could not be maintained. The temperature of the LiCor instrument typically had a diurnal range of 5-10K, and it was only recorded after DOY=36.7. Some authors [eg. *Elbers et al.*, 2001] have shown that the LiCor 6262 has a temperature dependent bias, giving lower mixing ratios at warmer temperatures [lower densities]. Consequently we made a density correction to the LiCor data, which typically increases afternoon mixing ration by about 2%. The comparison against the DPH instrument shows that this correction removes almost all the temperature bias.

4.3 Density correction of the LiCor 6262 Gas Analyzer and comparison against Dew point hygrometer.

The calibration we used to convert mV output from the GA to vapor pressure was made at the end of the experiment at 0905LT on Day 60 [March 1, 1999]. From pressure and LiCor temperature, we calculated density at the calibration time as 1.118. Density $\rho(p,T_{Licor})$ was calculated from MC pressure, p, and LiCor temperature T_{Licor}, and mixing ratio was scaled by density

$$Q_{GAcorr} = Q_{GA} * 1.118/\rho \qquad (1)$$

Since the LiCor temperature is a minimum at night and a maximum in late afternoon, this density correction typically slightly reduces the GA mixing ratio at night (a desirable impact since the uncorrected data often suggests slight supersaturation with respect to the thermister profile), and increases Q a little in the afternoon.
Figure 5 shows the mean diurnal cycles of T_{licor}, T_{ref}, and scaled density to give some appreciation of this correction.

T_{licor} was in fact only recorded after DOY=36.7, but fortunately it was reasonably well correlated with the temperature of the datalogger, T_{Ref}, which was recorded throughout the experiment. So we used the regression between the two temperatures

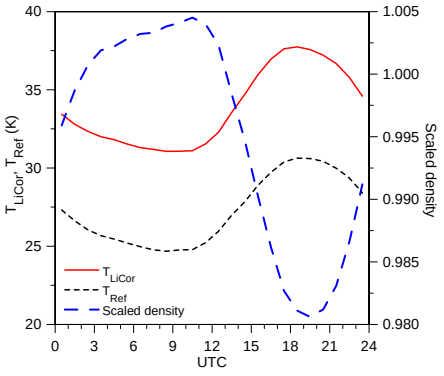

Figure 5. Mean diurnal cycle of T_{LiCor}, T_{ref} and scaled density.

$T_{licor} = 5(\pm 1.25) + 1.06(\pm 0.008) * T_{ref}$ ($R^2 = 0.84$)

to estimate T_{licor} (and hence density) for the earlier part of the experiment. An error of ±1K in T_{licor} corresponds to only ±0.3% in the density correction, which in turn represents a somewhat smaller correction in RH of ±0.2% for typical afternoon values of RH.

In the latter part of the experiment, for 38.635< DOY< 56.86, we have reliable data from both the dew-point hygrometer at 6m and the GA, so we show the difference between GA and DPH before and after the density correction of the GA data. First, we logarithmically interpolated the GA data from 4 and 9.5m to the 6-m level of the DPH instrument. Figure 6 shows the difference ΔQ at 6m between the LiCor GA (a 2-min sample every 10-min) and DPH (a 10-min average) as a function of scaled density at the LiCor temperature and pressure. Scaled density is ρ/1.118. The upper panel shows the increase with density (which is dominated by the dependence on temperature) of uncorrected GA Q relative to the DPH. The lower panel shows that after the density correction, most of this density dependence has been removed. However the data is banded: three bands are shown for different time intervals.
38.635<DOY<45.65
45.65<DOY<50.75
50.75<DOY<56.86

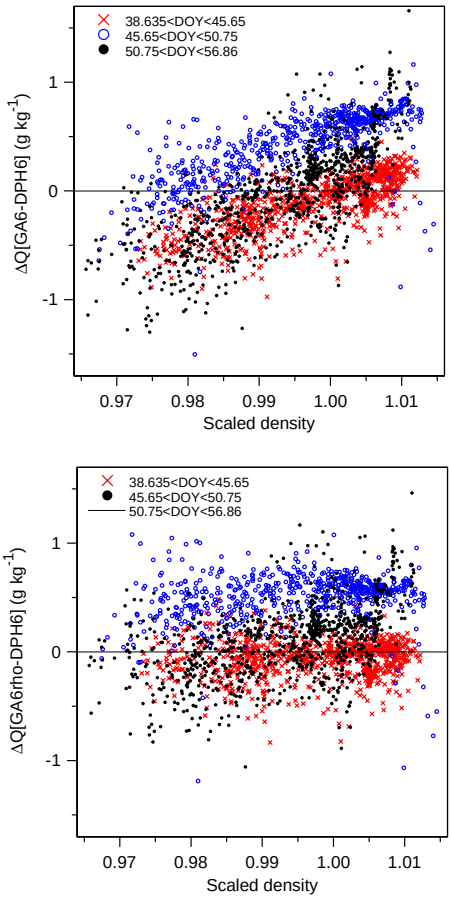

Figure 6. Difference between GA and DPH mixing ratio, Q, before (upper panel) and after density correction of the GA data (lower panel).

The offsets between the different bands in Figure 6 indicate that the relative calibration of the DPH instrument and the GA is not certain to ±0.3 gkg^{-1}, although the mean difference between the GA and the DPH over this period is small, ≈0.14g kg^{-1}. The offset for the period 45.65<DOY<50.75 appears to result from an adjustment made to the GA at 45.65, and a subsequent readjustment at 50.75. Beyond 56.86, the DPH instrument has an upward drift (not shown) so we have not included these data here.

4.4 Removal of RH biases between gas analyzer and (T, RH) probes.

We compared humidity in terms of pressure height to the lifting condensation or saturation level (P_{LCL}) , by calculating saturation temperature and pressure from mixing ratio and potential temperature, using the formulae in table 3.

Table 3. Thermodynamic formulae

Variable	**Formula used**
p [hPa] pressure	[Measured at 2m; hydrostatically corrected to other heights]
T [deg C] temperature	[Measured air temperature]
θ [K] potential temperature	(T + 273.15) * (1000 / p) ^ 0.286
Q [g kg^{-1}] mixing ratio	Computed from GA, (T, RH)-probe or DPH
T^* [K] : LCL saturation temperature	55+(2840/(3.5*LN(θ)-LN(1000*Q/(622+Q))-4.805))
p^* [hPa]: LCL saturation pressure	1000 * (T^*/θ) ^ 3.4965
P_{LCL} [hPa]	p-p^*
θ_E [K] equiv. pot. temperature	θ * EXP(2.67 * q / T^*)

We cannot compare relative humidity (RH) directly, since the RH6 sensor has the solar heating problem shown in Figure 3, which means that even if it is correctly measuring mixing ratio, its daytime RH is biased low simply because its temperature is biased high. (The tethersondes have a similar error in low winds). Figure 7 compares this derived variable P_{LCL}, which may be regarded as a surrogate for true RH (shown on right-hand scale to slight approximation of order 1%). This was calculated using the temperature profile sensors from Figure 1, as follows

a) For the GA values, it is computed from the potential temperature profile and the GA Q profile, so it corresponds to an RH relative to saturation at the temperature measured by the profile of thermisters. We assumed a logarithmic profile between 0.5 and 1.5m to derive the 1-m temperature and GA mixing ratio, and between 4 and 9.5m to derive the 6m GA mixing ratio.

b) For the (T, RH) probes P_{LCL} is computed from exactly the same 1-m and 6-m potential temperatures and the Q values calculated from the (T, RH) probes. This P_{LCL} thus corresponds also to RH relative to saturation at the thermister profile temperature.

In Figure 7 the gas analyzer curves (in black) corresponding to the three levels shown are very close in the daytime. Note that the GA data shows negligible mean gradient in P_{LCL} between 6 and 9.5m. However, the 1-m (T, RH) probe measurement (in red) is less saturated than the GA at the same level (by nearly 16 hPa or -5% in RH) and the 6-m (T, RH) probe measurement (in blue), is measuring a Q that is closer to saturation than the GA at the same 6-m level by about -7.5 hPa (equivalent to +2.5% in RH). These are large biases.

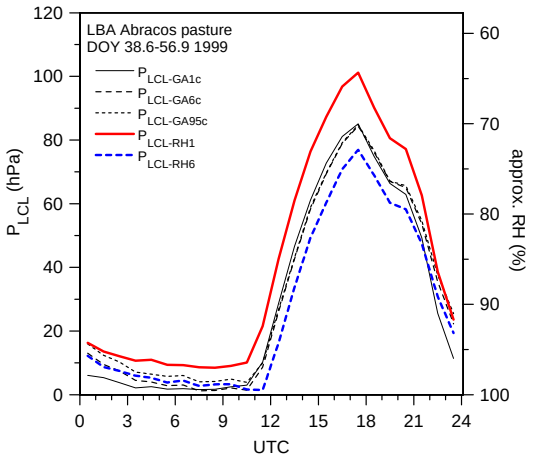

Figure 7. Comparison of mean diurnal cycle of P_{LCL} from GA (corrected) and RH-probes (uncorrected).

Figure 8 shows scatter plots from the 10-min data. The left panel shows P_{LCL}(GA6c) against P_{LCL}(GA1c), together with the 1:1 line. Some of the scatter will be related to the non-synchronous sampling at the two levels. However, the plot confirms that there is little systematic variation in

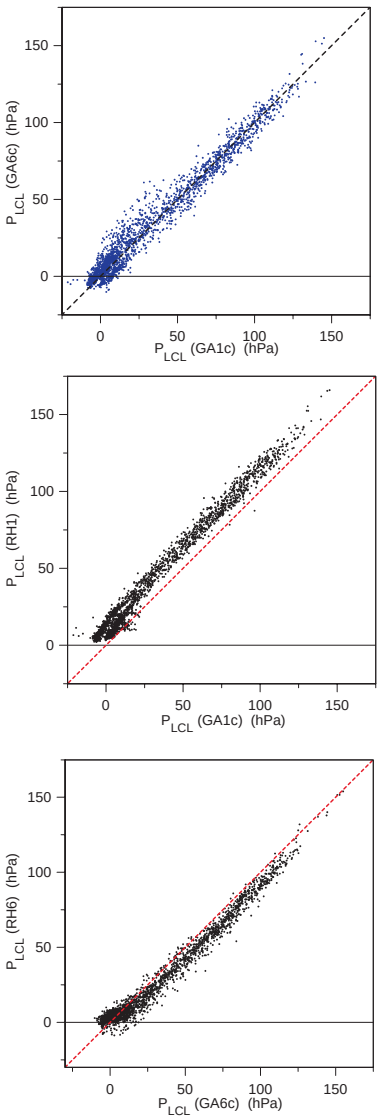

Figure 8. Density corrected GA P_{LCL} at 6m against 1m (upper panel). MC P_{LCL} at 1m against GA at 1m (middle) and same comparison at 6m (lower).

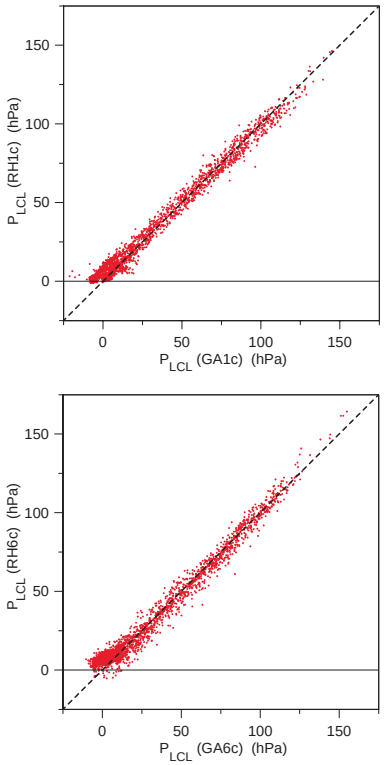

Figure 9. Bias corrected P_{LCL} from RH-probes plotted against GA P_{LCL} for 1m (upper panel) and for 6m (lower).

P_{LCL} between the two levels. There is a little banding near the origin which corresponds to times at night
later in the experiment when the gas analyzer tubes were heated to reduce problems with condensation (one band is DOY# 53-57.6). The middle panel plots P_{LCL}(RH1) against P_{LCL}(GA1c) for the same level, which shows that the dry bias of this sensor is quite systematic. The third panel shows that the corresponding moist bias of the RH6 sensor is also quite systematic and therefore could be removed (despite the ventilation issue). We chose a simple procedure to remove these relative humidity biases. We defined
$\Delta RH = \Delta RH_x$ a fixed correction for RH<85%, and
$\Delta RH = \Delta RH_x - \Delta RH_y * (RH-85)/15$ a linear correction for 85<RH< RH_{max}
The value near saturation was determined to adjust RH_{max} to 100%. The value for RH<85 was chosen to give no mean bias in P_{LCL} for the (mainly) daytime period 9-19LT between the GA and RH instruments at 1m; and between RH and the mean of the GA and DPH instruments at 6m. The resulting corrections shown in Table 4 were applied to the data, giving the corrected scatterplots shown in Figure 9, with the suffix C on the data derived from the RH sensor to indicate corrected data. The reduction in the bias in comparison with the corresponding plots in Figure 8 is apparent.

Table 4. Bias corrections for RH sensors

	RH1 sensor	RH6 sensor
ΔRH_x	5	-2.1
ΔRH_y	4	-0.7

After applying these corrections the mean diurnal cycle comparison for Q and P_{LCL}, corresponding to the 1- and 6-m levels in Figures 4 and 7 are shown in Figures 10 and 11. There is now correspondence in the

mean diurnal cycles of mixing ratio at the two levels to about 0.1 g kg^{-1} in the daytime, far better than in Figure 4. The only exception is the RH6 sensor which has a morning peak that is about 0.4 g kg^{-1} too high in comparison to the GA and DPH data which are close. This is caused we believe by the ventilation problem as the sensor RH drops too slowly from saturation at sunrise. In this average the GA data is a little wetter than the DPH data, and at night the GA is also higher. However the GA instrument had problems with condensation in the lines at night, and the lines were heated after DOY= 46.19. We still consider the GA data to be less reliable at night as some values of Q_{GA} at night are slightly supersaturated with respect to the thermister profile.

The agreement in the diurnal cycle of P_{LCL} with the gas analyzer data and DPH data is now extremely close in the daytime (compare Figure 7), except for the lag of the RH6 sensor after sunrise.

Since the values of P_{LCL} in Figure 11 were calculated using the same temperatures (measured by the thermister profile), the close agreement in daytime P_{LCL} to better than ±3 hPa, means than we can reduce the *relative mean* biases in RH between the sensors to better than ±1% in RH, far better than the biases shown in Table 4. The RMS difference between MC and GA data is about 0.4 g kg^{-1}, but the sampling of the two datasets is different. The GA data is sequential 2-min samples in each 10-min, followed by an interpolation between adjacent levels, while the MC data is a true 10-min mean.

Our absolute accuracy is tied to the accuracy of the GA calibration using a dew point generator. The offsets between the different bands in Figure 6 indicate that the relative calibration of the DPH instrument and the GA is not certain to ±0.3 gkg^{-1}, although the mean difference between the GA and the DPH over this period is small, ≈0.14g kg^{-1}. We conclude that the absolute accuracy of the corrected Q data is probably ±1-2% in RH.

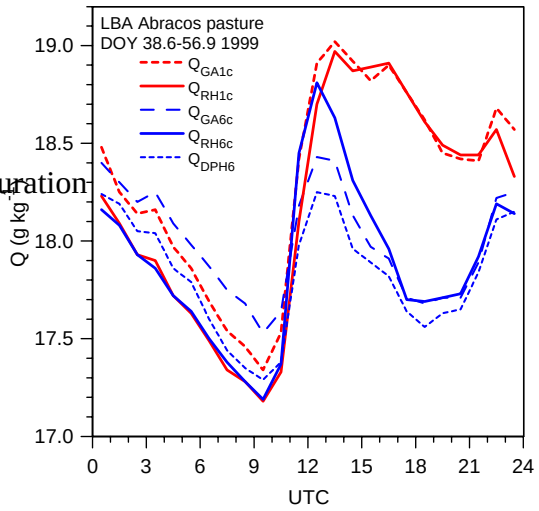

Figure 10. Comparison of corrected mean diurnal cycles of Q at two levels.

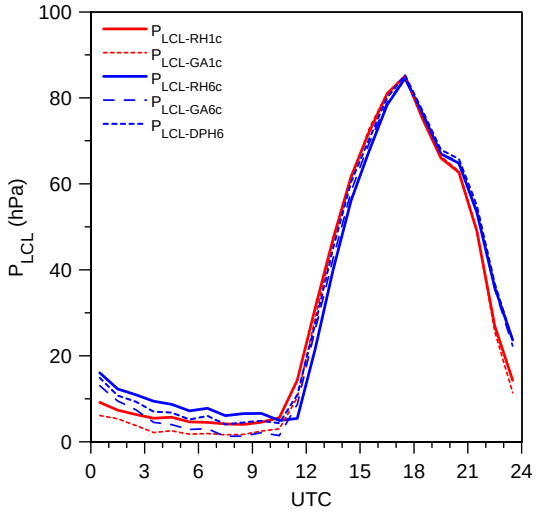

Figure 11. As Figure 10 for corrected P_{LCL}.

5. Comparison of Micromet and tethered balloon

5.1 Mode of operation of tethered balloon, time correction and data filtering

Ascent/descent profiles were made by the tethered balloon (TB) every 3h to coincide with each rawinsonde launch, usually starting 30min before the nominal launch times of 00, 03, 06, 09, 12, 15, 18, and 21 UTC. The sonde was tethered at 10m, the height of the top of the tower, for 10mins before and after each ascent/descent profile for cross-calibration against the micromet tower. The TB sonde sampled

every 2 s, so 30 samples were averaged to 1-min for comparison with the 1-min micromet data. The 10-min "calibration runs" were each checked carefully by comparing visually pressure, wind, temperature and humidity to ensure sonde biases were based on times when the sonde was properly exposed and moored near 10m. Sonde biases were determined relative to the tower for each of the three tethersonde packages used during the experiment:

SOND#1 21 < DOY < 24.75 [balloon lost]
SOND#2 24.75 < DOY <55.56 [instrument failure]
SOND#3 55.56 < DOY < 60

For the last period with SOND#3, the tether height for these calibration runs was reduced to 6m, so the comparisons for pressure and temperature are made with the tower at this level.

5.1.1 Clock difference

The micromet tower and the tethersonde had different datalogger clocks and it appears that the time on the TB data is about 1 min behind that of the MC data, based on the regression of the TB wind velocity with the MC wind velocity, which gave a maximum R^2 correlation for a lag of 1min, as shown in Table 5. We corrected the TB clock by 1 min to the timebase of the MC data.

Table 5. Regression of tethered balloon WV on micromet WV as a function of time difference.

Time-lag: MC-TB [min]	0	1	2	3
R^2 correlation	0.871	0.905	0.831	0.778

5.1.2 Filtering of the tethersonde data for solar heating in low wind-speeds

Before averaging to 1-min, the TB data was first filtered to remove 2sec data points with low windspeeds during daylight hours, to remove a solar heating bias on the temperature sensor when poorly ventilated [Heitz, 2001]. The criterion for rejection of 2-sec data was

[Wv] < 1.5 ms-1, between times 0900 to 1530 LST
[near local noon]
[Wv] < 1.0 ms-1 , between times 0630 to 0900 LST and 1530 to 1730 LST.

These criterion are based on the MS study of Heitz [2001], who noted the warm bias at high radiation levels and low winds <1.5m/s. In general we do not have radiation levels on the sensor as the balloon goes up, so I have applied a criterion based on time of day and wind only. Some small solar bias remains, as I used a lower wind threshold around sunrise and

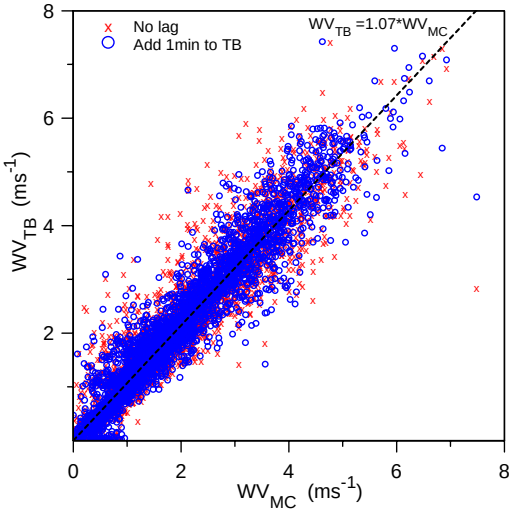

Figure 12. Wind-speed comparison between TB and MC with and without a 1-min timelag.

sunset. An additional wind based correction will be derived later (section 5.4.2) The 1-min dataset includes a counter field, K-min, to indicate the number of 2 sec. data points included in a 1-min average.

5.2 Wind comparison

5.2.1 Wind-speed comparison

Figure 12 shows the WV_{MC} with and without the 1-min timelag, plotted against WV_{TB}, showing that the scatter is somewhat reduced. The regression line through the origin for timelag 1 min is

WV_{TB} =1.070 (±0.003) WV_{MC}

with an R^2 =0.905. The TB windspeeds are about 7% higher than the tower measurements at 10m. Part of this could be due to the possibility that the tethersonde package may be a few meters above the tower on many occasions. We made no correction for this difference.

5.1.3 Wind direction comparison

The tethersonde sensor measures wind direction relative to magnetic north. At the Rondônia pasture site the magnetic variation is -11°, that is, magnetic north is 11° west of true north, so that the wind direction measured with respect to magnetic north is larger than from true north. The tower instrument was aligned to magnetic north using a compass.

The three sondes have significantly different mean difference in wind direction from the tower microclimate sensor, as shown in Table 6 for wind-speeds>1 ms^{-1}. Note that there is much more data for SOND#2. Clearly not all these measurements can be from magnetic north. Since the sondes vary by ± 16 relative to the fixed tower, we treated the tower as the reference, and corrected the 3 tethersondes to it.

Table 6. Mean difference in wind direction [MC-TB] as a function of wind-speed.

WV range (ms-1)	SOND#1	SOND#2	SOND#3
1 to 2	13.8	-18.7	-7.0
2 to 3	17.9	-17.2	-8.6
3 to 4	16.6	-16.2	-8.0
4 to 5	17.3	-18.1	-8.3
Mean	16.2±8.5	-17.8±11.5	-7.9±15.2

Figure 13 shows the scatter plot of wind direction (for wind speeds

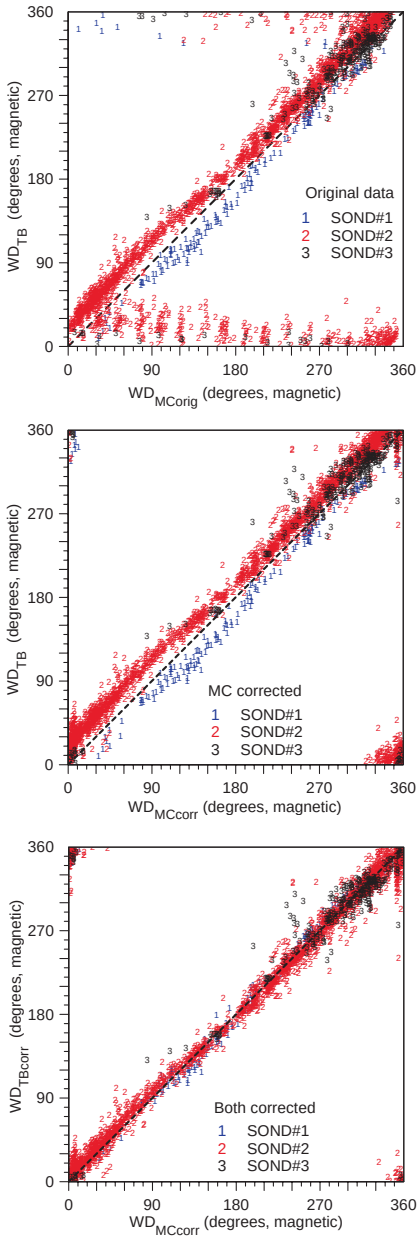

Figure 13. TB wind direction against MC wind direction for original data, corrected MC and both corrected.

>1 ms^{-1}) between the two systems for the three sondes for the three stages of our correction: the upper panel for the raw data (in which the MC data has the WD errors from averaging, discussed in section 3.1.2; the middle panel with the corrected MC data, showing the banding from the three different TB Sondes, before correction, and the lower panel after applying the biases from Table 6. This figure shows magnetic wind directions. In the data set, we have also added wind direction from true north.

5.3 TB-MC pressure comparison.

Table 7 shows the mean/SD of the difference between the microclimate pressure sensor, extrapolated hydrostatically to 10m [6m for SOND#3], and the pressure sensor on each tethersonde, partitioned into night-time and daytime.

Table 7. Δp (MC-TB) (hPa)

	SOND#1	SOND#2	SOND#3
Night	0.80±0.33	1.22±0.35	0.67±0.38
Day	0.60±0.24	1.15±0.25	0.51±0.13

The mean difference is a little larger at night implying that the sonde was 1-2m higher on average at night [if the pressure sensors have no temperature dependent bias], and the standard deviation is larger at night implying that accurate tethering of the package at 10m was a little more difficult at night. Consequently we used the daytime differences as corrections [added to the TB pressure], on the grounds that the TB sonde was moored closer to 10m in the daytime. The standard deviation corresponds to a relative height fluctuation between TB sonde and top of the tower of 2-3m in the daytime.

5.4 TB-MC temperature comparison

5.4.1 Temperature bias correction.

Before averaging up to one-min, the data was filtered, as discussed in section 5.1.2 to reduce solar heating errors in low winds. Table 8 shows the mean/SD of the difference between the MC T_{air95} [T_{air60} for SOND#3] and the TB temperature, partitioned into night-time and daytime, based on incoming SW radiation, < >10 Wm-2 .

Table 8. ΔT (MC-TB) (K)

	SOND#1	SOND#2	SOND#3
Night (<10 Wm-2)	0.02±0.23	0.23±0.19	0.54±0.14
Day (>10 Wm-2)	0.20±0.42	0.33±0.33	0.89±0.34

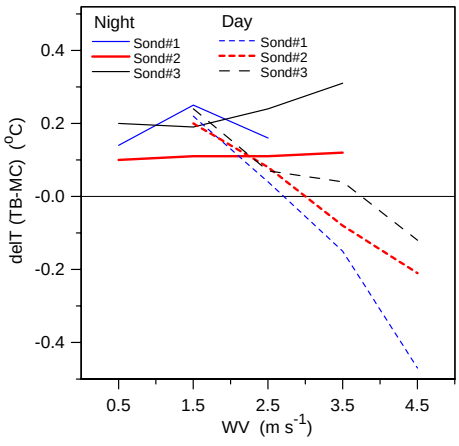

Figure 14. ΔT_{TB-MC} binned by wind-speed, and partitioned into day and night by incoming solar radiation.

The mean differences and standard deviations are smaller at night, which is consistent with the atmosphere being stably stratified and the tethersonde being on average slightly higher at night [where it is warmer]. Again we used the daytime differences as more representative corrections, and added them as bias corrections to the TB temperatures.

5.4.2 Daytime correction in low winds

After applying these bias corrections, the residual difference between TB and MC temperatures [note sign here is TB-MC] is shown in Figure 14, stratified by wind-speed, and partitioned into day/night. The TB-sondes at night are warmer, consistent with Table 8. In the daytime, the mean difference is zero, since this was the basis of the correction, but there is a significant wind-speed dependent bias. At low wind-speeds, the TB is warmer – this could be some residual heating of the sonde, which we have not filtered out. However the cold bias of the sonde at high wind speeds, when it is well ventilated is a little puzzling. One reason may be the gradient of temperature in the superadiabatic layer: if the sonde height is a few meters above the tower, then its temperature will be a little colder. [From the pressure sensor there appears to be no systematic variation in relative height with wind-speed]. So on this basis, we applied the following bias correction as a function of wind-speed.

$\Delta T_{vent} = 0.15*(Wv-4)$ for $SW_{down} > 100$ and $1 < Wv < 4$

This gives a negative correction for daytime data, which reaches a maximum value of -0.45 at 1ms^{-1}, and is zero for Wv>4 and for low incoming solar radiation. Careful examination of the data did not justify a radiation dependent correction, perhaps because the impact on the sensor is sensitive to solar elevation angle. Figure 15 shows the impact of this correction on SOND#2, for which we have the most data. Three sets of lines are shown. The solid lines are the difference ΔT_{cTB-MC} , after applying the bias corrections from Table 8, stratified by solar radiation level into "Night" for SW<10 Wm $^{-2}$ and two daytime ranges 10<SW<500 and SW>500 Wm^{-2}. We show only 2 broad daytime ranges, since a finer stratification (not shown) does not indicate a clear trend. The dotted lines are the corresponding mean ΔT on the tower between 9.5m and 6m.

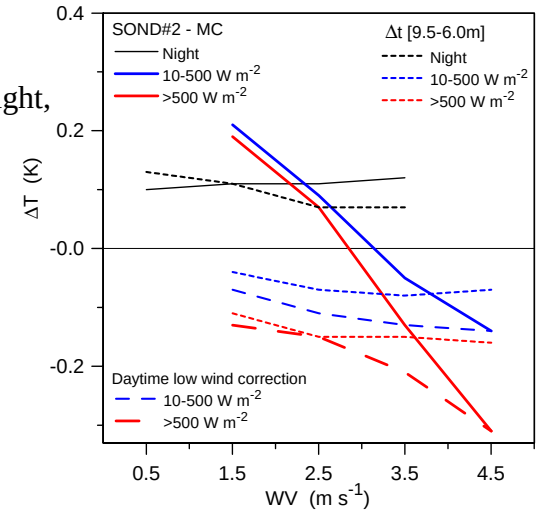

Figure 15. ΔT_{TB-MC} for SOND#2, binned by wind-speed and solar radiation: see text.

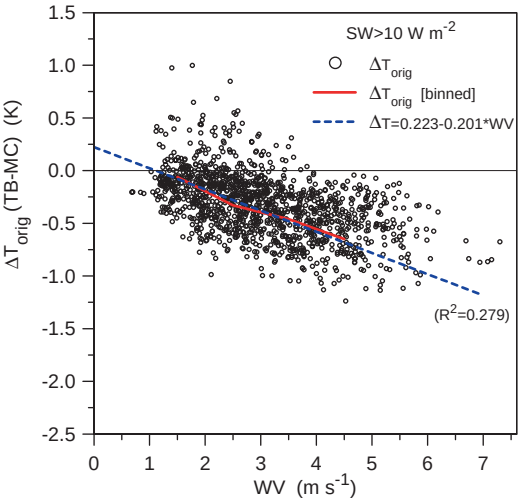

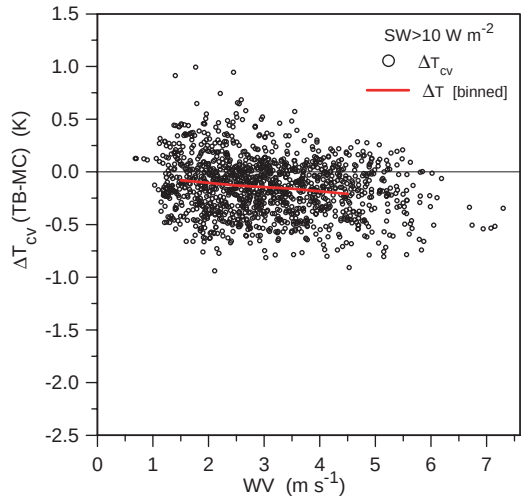

Figure 16. Scatterplot of daytime ΔT_{TB-MC} against wind-speed, with and without correction for low ventilation.

We show these as closely representative of the expected temperature difference between sonde and the 9.5m level on the tower, if the sonde is at 13m. They show the stable stratification at night and the superadiabatic layer in the daytime, increasing in strength with solar radiation. The dashed lines show ΔT_{cw} (TB-MC) after adding the correction ΔT_{vent} for the solar heating at low wind-speeds (this correction is zero above 4ms^{-1}). Most of the slope with wind speed is removed (except at high wind-speeds), and the residual differences is generally consistent with an increasing superadiabatic layer at higher solar irradiance, and a few meters height difference between TB and the top of the tower.

Figure 16 shows a daytime (SW>10 W m^{-2}) scatterplot of ΔT_{TB-MC} for the original data (above), and after applying the bias and wind dependent corrections for SOND#2 (below). The heavy red curves come from binning the data in 1 ms^{-1} ranges, and on the upper panel we have also added (dashed) the regression line. Most of the wind dependent bias has been removed.

5.5 P_{LCL} and humidity bias correction

As in earlier sections we first intercompared TB-sonde and MC humidities in terms of saturation level, and then corrected RH to reduce the bias in $P_{LCL.}$ Recall from section 4.4, Figure 7, that the GA data showed negligible mean gradient in P_{LCL} between 6 and 9.5m, so our comparisons between the TB at 10m and the 6m data in P_{LCL} should indicate instrumental biases, uncontaminated by any gradient with height. We treated the pressure correction and the bias temperature correction to the TB sensor as instrumental offsets, and applied these before computing mixing ratio q. However, as with the 6m sensor on the tower, we assumed the temperature error caused by poor ventilation did not yield an error in q. Consequently, P_{LCL} for the TB was calculated from q, before applying the ventilation correction for temperature and from θ, after correcting for poor ventilation. These initial biases in P_{LCL} , shown in Table 9, lines 1 and 2, are large for SOND#2 and #3, corresponding to the sondes having higher relative humidities of nearly 6 and 7% respectively, relative to the (corrected) 6m sensor, whose RH was reduced by 2.1% (see Table 4).

Table 9. ΔP_{LCL} (MC_{6mcorr}-TB) (hPa) after TB bias corrections, and after applying ΔRH_s correction.

Correction	Filter	SOND#1	SOND#2	SOND#3
TB bias corrected	Night	3.9±5.3	7.7±4.1	9.2±3.9 [hPa]
TB bias corrected	Day	-0.1±7.4	14.7±7.5	20.0±9.4 [hPa]
With ΔRH applied	Day, RH<90%	0±7.5	0.1±7.3	0±8.7 [hPa]
ΔRH_s [%]		0	-5.7	-6.8 %

The sonde data had already been truncated to 100%, so we could not determine an offset correction at high humidities. Consequently, the correction procedure we adopted is simpler than that used in section 4.4. We selected the daytime data with RH<90% and defined a correction ΔRH_s for each sonde, that reduced the daytime mean difference of P_{LCL} to zero. Above 90% RH, this correction was scaled to zero at 100%, $\Delta RH = \Delta RH_s * (RH-90)/10$.

The bottom line in Table 9 shows the ΔRH_s corrections and the line above shows the corrected mean differences in ΔP_{LCL} (MC_{6mcorr}-TB), filtered to the daytime data and for RH<90%.

Figure 17 shows the scatterplot of P_{LCL} before and after correction of the tethersonde data. Most of the bias against the tower data has been removed after correction, although some points for SOND#3 are outliers. The standard deviation of ±7-8 hPa in Table 9 corresponds to ± 2-3% in RH. Note that the correction method is unsatisfactory at low winds during daytime (see negative P_{LCL} in lower panel), when the sonde RH=100%, because the wind correction reduces temperature, but RH remains uncorrected at 100%.

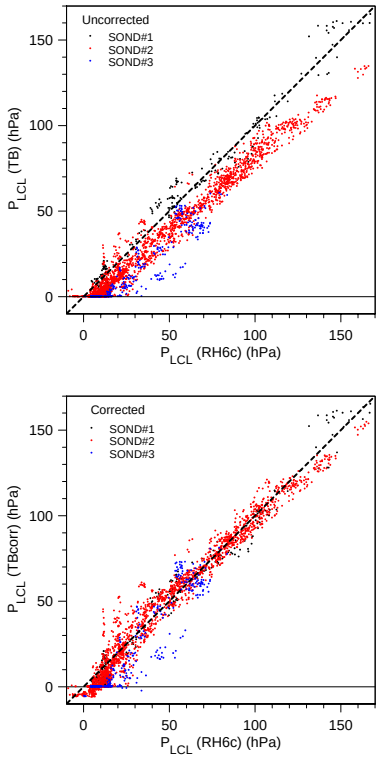

Figure 17. Scatterplot of P_{LCL} for TB against 6-m MC before and after correction of sonde data.

6. Summary and conclusions

This document summarizes the calibration and correction of the LBA/TRMM data set collected at the Abracos pasture site at Ouro Preto d'Oeste, Rondônia, Brazil in January and February, 1999 as part of the WETAMC campaign. To summarize what we have accomplished:

a) Wind direction

We have corrected wind direction errors in the surface MC data and the TB data [and the rawinsonde data, discussed elsewhere]. The merged TB_MC data contains wind direction, relative to both magnetic and true north; while the other datasets have only corrected MC wind relative to magnetic north.

b) Pressure

We have corrected small differences in pressure between MC and TB.

c) Temperature

We have referenced the TB sondes to the thermisters on the MC tower, and corrected a daytime, low-wind [ventilation] bias for the TB data. However we have no absolute reference for temperature, and some uncertainty remains in the low ventilation correction.

d) Humidity, mixing ratio and height to saturation level, P_{LCL}.

The primary purpose of this experiment design was to cross-calibrate humidity sensors and reference them back to a calibrated gas analyzer, since accurate humidity measurements have long been difficult, especially in the tropics and in the rainy season. In this we have been largely successful. A density correction to the GA data removed almost all its temperature [and pressure] dependence relative to a calibrated DPH. We have reduced the relative mean biases between different sensors [MC, GA and DPH] to about ± 1%. There remain some uncertainties in the absolute calibration of both GA and DPH instruments against a dew point generator reference standard. Consequently, we believe that the absolute calibration accuracy of the humidity data may only be ±1-2% in RH. This is however far superior to the

accuracy of conventional RH sensors. Table 10 shows the corrections applied to the different sensors to reference them to the corrected GA data.

No correction was applied to the DPH data which in the mean differed from the corrected GA data by <0.5% equivalent RH. However, Figure 6 shows that during February, the relative calibration of these two instruments shifted by ±0.3 g kg^{-1}, roughly equivalent to ±1-2% in RH.

Figure 18 shows the mean diurnal cycle for a 7-day period (DOY 39-45) for mixing ratio, Q, pressure height to LCL, P_{LCL}, and finally equivalent potential temperature, θ_E. The upper panel of Q shows the regular progression of mixing ratio from the GA from 0.5m to 9.5m. The 1m data and 6m data from different sensors now fit this progression, except for the overshoot of the 6m RH sensor (due to poor ventilation). The middle panel of P_{LCL} shows the close agreement at all levels, apart from the lag of the RH6 sensor at 1200UTC in leaving its pre-dawn saturation. The slightly higher values of P_{LCL} for the DPH instrument near 1500 are in fact only a sampling problem: some DPH data is missing. Clearly the estimation of daytime cloud-base height and mixed layer depth is not very sensitive to the choice of data level until the late afternoon. The lower panel of θ_E shows that, while there is a strong peak close to the surface at local noon, the gradient of θ_E is small between 6 and 9.5m, and the daytime rise at these levels is much reduced. (Again we can see the morning overshoot problem of the RH6 instrument). Clearly the 6 or 9.5m levels should be used to estimate BL θ_E for the estimation of convective available potential energy.

An error of ± 1% in RH near noon, corresponds to ±3 hPa in cloud-base and to slightly less than ±1K in θ_E. This is now the mean relative accuracy of the humidity instruments, while the absolute accuracy may be slightly poorer.

In summary, this corrected dataset is extremely valuable for the study of boundary layer and convective processes over Rondônia in the rainy season.

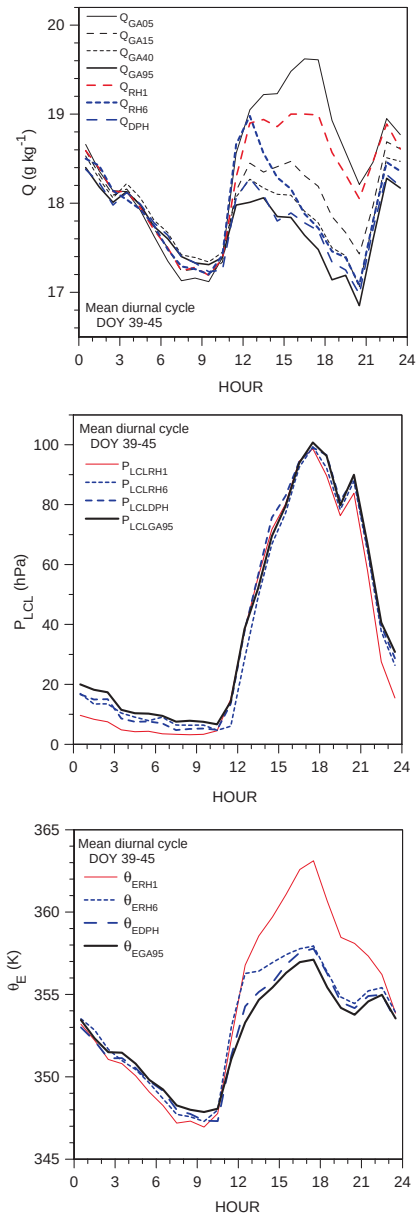

Figure 18. Diurnal cycle of Q, P_{LCL} and θ_E at different levels from different instruments after correction.

Table 10. RH corrections applied to different sensors.

Sensor	GA [density corrected]	DPH6m	RH1m	RH6m	SOND#1	SOND#3	SOND#3
ΔRH (%)	[standard]	[<0.5]	+5	-2.1	0	-5.7	-6.8

Acknowledgments.

This LBA data collection was supported by a NASA-TRMM grant to the University of Virginia. Alan Betts is supported by NASA under grant NAG5-8364, and by NSF under Grant ATM-9988618.

References

Betts, A. K., J. Fuentes, M. Garstang, and J. H. Ball, 2002a: Surface diurnal cycle and Boundary Layer structure over Rondônia during the rainy season, *J. Geophys. Res.*, **107**, in press, LBA special issue.

Betts, A. K., L.V. Gatti, A.M. Cordova, M. A. F. Silva Dias, and J. Fuentes, 2002b: Transport of ozone to the surface by convective downdrafts at night. *J. Geophys. Res.*,**107**, in press, LBA special issue.

Betts, A. K. and C. Jakob, 2002, Evaluation of the diurnal cycle of precipitation, surface thermodynamics and surface fluxes in the ECMWF model using LBA data.. *J. Geophys. Res.*, **107**, in press, LBA special issue.

Elbers, J. A., A, C. de Araujo, P. Stefani, P. J. de Oliveira, and B. Kruijt, 2001, How accurate is latent heat flux from Licor LI-6262 measurements under tropical conditions? Poster from Alterra Green World Research, Department of Water and the Environment, PO Box 47, 6700 AA Wageningen, the Netherlands, J.A.Elbers@alterra.wag-ur.nl

Heitz, R. C. H., 2001, Mixed layer budgets and entrainment rates of heat and water vapor over a deforested site in Amazonia., M.S Thesis, Dept. of Environmental Sciences, Univ., of Virginia, Jan, 2001, 160pp.

Silva Dias, M. A. F., W. Petersen, P.L. Silva Dias, R. Cifelli, A.K. Betts, M. Longo, A.M. Gomes, G.F. Fisch, M.A. Antonio, and R.I. Albrecht, 2002: A case study of convective organization into precipitating lines in the Southwest Amazon during the WETAMC AND TRMM-LBA. *J. Geophys. Res.*, **107**, in press, LBA special issue.

Williams, E. and 32 Co-authors, Contrasting Convective Regimes Over the Amazon: Implications for Cloud Electrification, *J. Geophys. Res.*, **107**, in press, LBA special issue.

List of Figures.